



## Characterization of acyl carrier protein and LytB in *Babesia bovis* apicoplast

Marina C. Caballero<sup>a</sup>, Monica J. Pedroni<sup>b</sup>, Guy H. Palmer<sup>a</sup>, Carlos E. Suarez<sup>a,b</sup>,  
Christine Davitt<sup>c</sup>, Audrey O.T. Lau<sup>a,\*</sup>

<sup>a</sup> Program of Genomics, Department of Veterinary Microbiology and Pathology and Paul G. Allen School for Global Animal Health, College of Veterinary Medicine, Washington State University, Pullman, WA 99164-7040, USA

<sup>b</sup> Animal Disease Research Unit, Agricultural Research Service, United States Department of Agriculture, Pullman, WA 99164-6630, USA

<sup>c</sup> Franceschi Microscopy and Imaging Center and the School of Biological Sciences, Washington State University, Pullman, WA 99164-4210, USA

### ARTICLE INFO

#### Article history:

Received 4 September 2011

Received in revised form 12 October 2011

Accepted 18 October 2011

Available online 25 October 2011

#### Keywords:

Apicomplexan

Apicoplast

*Babesia bovis*

*Plasmodium falciparum*

FASII

MEP

ACP

LytB

### ABSTRACT

The apicoplast is a highly specialized organelle that mediates required functions in the growth and replication of apicomplexan parasites. Despite structural conservation of the apicoplast among different parasite genera and species, there are also critical differences in the metabolic requirements of different parasites and at different stages of the life cycle. To specifically compare apicoplast pathways between parasites that have both common and unique stages, we characterized the apicoplast in *Babesia bovis*, which has only intraerythrocytic asexual stages in the mammalian host, and compared it to that of *Plasmodium falciparum*, which has both asexual intraerythrocytic and hepatic stages. Specifically focusing on the type II fatty acid (FASII) and isoprenoid (MEP) biosynthesis pathways, we searched for pathway components and retention of active sites within the genome, localized key components [acyl carrier protein (ACP) and 4-hydroxy-3-methylbut-2-enyl diphosphate reductase (LytB)] to the apicoplast, and demonstrated that the N-terminal bipartite signals of both proteins are required and sufficient for trafficking to the apicoplast lumen. Using specific pharmacologic inhibition, we demonstrated that MEP biosynthesis may be disrupted and its presence is required for intraerythrocytic growth of *B. bovis* asexual stages, consistent with the genomic pathway analysis and with its requirement in the asexual erythrocytic stages of *P. falciparum*. In contrast, FASII biosynthesis may or may not be present and specific drug targets did not have any inhibitory effect to *B. bovis* intraerythrocytic growth, which is consistent with the lack of requirement for *P. falciparum* intraerythrocytic growth. However, genomic analysis revealed the loss of FASII pathway components in *B. bovis* whereas the pathway is intact for *P. falciparum* but regulated to be expressed when needed (hepatic stages) and silent when not (intraerythrocytic stages). The results indicate specialized molding of apicoplast biosynthetic pathways to meet the requirements of individual apicomplexan parasites and their unique intracellular niches.

© 2011 Elsevier B.V. All rights reserved.

### 1. Introduction

The existence of a multi-membranous apicoplast within the phylum Apicomplexa was first observed in the 1960s and subsequently identified as a promising chemotherapeutic target due to its eubacterial and plant-like properties [1,2]. The apicoplast is the result of two separate endosymbioses with the engulfment of a cyanobacterium and an alga during the primary and secondary endosymbioses, respectively [3–5]. Within this organelle, two apicoplastic pathways, FASII and non-mevalonate 1-deoxy-D-xylulose-5-phosphate (DOXP) isoprenoid (MEP) biosyntheses, were identified and extensively investigated. Products from the

FASII pathway participate in energy production and cell structure maintenance. Among the major components of the FASII pathway, acyl carrier protein (ACP) functions by holding the growing fatty acid chain covalently via its phosphopantetheine prosthetic group [6]. Thus, ACP is often used as a positive marker of apicoplast luminal protein for *Plasmodium* and *Toxoplasma* [7,8]. However, ACP is also found in mitochondria in plants and organisms such as *Neurospora* sp. as it forms part of the respiratory chain complex of NADH:ubiquinone oxidoreductase [9,10]. Thus, ACP can have dual functions. MEP biosynthesis is utilized exclusively by bacteria, Apicomplexan parasites, and plants as an alternative to the classic cytosolic mevalonate-dependant (MAD) mechanism, to produce isoprenoid precursors such as isopentenyl pyrophosphate (IPP) and dimethylallyl pyrophosphate (DMAPP) [11] which are involved in protein prenylation, cell membrane maintenance, protein anchoring and N'-glycosylation [12]. In this pathway,

\* Corresponding author. Tel.: +1 509 335 6072; fax: +1 509 335 8529.

E-mail address: laua@vetmed.wsu.edu (A.O.T. Lau).

4-hydroxy-3-methylbut-2-enyl diphosphate reductase (LytB, also known as IspH), catalyzes the final step of IPP and DMAPP production [13].

Characterization of FASII and MEP biosyntheses, mostly performed in *Plasmodium* and *Toxoplasma*, illustrates the crucial role in parasite survival [7,14]. Recent data reveal that not all apicomplexans are the same. Yu et al. and Vaughn et al. reported that FASII pathway is crucial only during the latter half of the liver stages in *Plasmodium falciparum* as it is not necessary during the mosquito and asexual erythrocytic stages [14,15] while *Toxoplasma* and *Eimeria* utilize both FASI and II for fatty acid production in the cytoplasm and apicoplast, respectively [16,17]. The *in silico* prediction of the lack of a FASII pathway in *Babesia bovis* [18], which lacks a liver stage but shares with *P. falciparum* asexual stage growth and replication within mature erythrocytes, further raises the question as to how ancestral apicomplexan pathways have been molded to meet the specific needs of parasite species.

In the present study, we used four linked approaches to identify and characterize the apicomplexan and two participants in FASII and MEP pathways in *B. bovis*: (i) visualization of the *B. bovis* four membrane apicomplexan in the asexual stage; (ii) identification and localization of ACP and LytB; (iii) testing the role of the bipartite targeting signals in trafficking to the apicomplexan lumen; and (iv) testing the sensitivity of the FASII and MEP pathways to specific pharmacologic inhibition. The results are presented and discussed in the context of these apicomplexan pathways among Apicomplexan parasites, with specific comparison between *Plasmodium* and *Babesia*, two genera of parasite that infect erythrocytes as asexual stages.

## 2. Materials and methods

### 2.1. Parasite strain and in vitro cultivation of *B. bovis*

The Mo7 biological clone of *B. bovis* was derived by limited dilution of a Mexico strain as previously described [19,20]. Parasites were grown in long-term microaerophilous stationary-phase culture [21,20] followed by expansion cultures [22] using previously described techniques.

### 2.2. RNA isolation and cDNA generation

Total RNA was isolated from *B. bovis* cultures using TRIzol (Invitrogen), treated with RNase inhibitor (Roche) and RNase-free DNase (Turbo DNA-free from Ambion) for 30 min at 37 °C. RNA was reverse transcribed with RETROScript kit (Ambion) using oligo-dT primers, according to the manufacturer's instructions for a 2-step RT-PCR.

### 2.3. Identification and cloning of *B. bovis* *acp* and *lytB* genes

*B. bovis* acyl carrier protein gene (*acp*) specific primers were designed based on a sequence extracted from accession number NW.001820857. Full length *Bb*acp forward and reverse primers were 5'-ATG AAC GTT GTA TTC CGT ATG CTT AAC-3' and 5'-TCA GAT GTC TTG TCG ACG TTC TAG CTT-3', respectively. *Acp* was amplified from *B. bovis* cDNA using SuperTaq Polymerase (Ambion). PCR conditions were 95 °C for 3 min for 1 cycle followed by 94 °C for 30 s, 55 °C for 30 s, 72 °C for 2 min for a total of 30 cycles, and a final elongation step at 72 °C for 5 min. Amplified PCR product was visualized by electrophoresis and subsequently cloned into a pCR®4-TOPO® vector (Invitrogen), following the manufacturer's protocol. Individual clones were selected, sequenced and analyzed (MacVector version 11.1). *LytB* specific primers were designed based on a sequence extracted from accession number NW.001820857. Full length *lytB* forward and reverse primers were 5'-ATG CTA AAA TTA TTA TTT TTA ATA CTG-3' and 5'-TTA TGT GCT GAC ACC CGG GC-3',

respectively. *LytB* was amplified from *B. bovis* cDNA cloned and sequenced using the same conditions as described above for *acp*.

### 2.4. 5' and 3' Rapid Amplification of cDNA Ends for *acp* (RACE)

Total RNA was used as the template to generate 5' RACE-Ready cDNAs by following the manufacturer's instructions (SMARTer RACE cDNA amplification kit, Clontech). Gene-specific primers with a Tm higher than 65 °C were designed. *Acp* RACE forward primer was 5'-ATG CTT AAC CCA TTG GGT ATT GCC TTT GTA GTC ATT CTA GCG C-3'. PCR was performed using Advantage 2 PCR kit (Clontech). Cycling conditions were: 94 °C for 30 s and 73 °C for 3 min for a total of 5 cycles; 94 °C for 30 s, 68 °C for 30 s and 72 °C for 3 min for 25 cycles, followed by 15 cycles of 94 °C for 30 s, 50 °C for 30 s, 72 °C for 2 min, and a final elongation step at 72 °C for 10 min. Amplified PCR products were confirmed by electrophoresis and corresponding bands were excised from the gel, purified using QIAquick Gel Extraction Kit (Qiagen) and subsequently sequenced.

### 2.5. Expression of recombinant mature *Babesia bovis* ACP and LytB

Determination of the acyl carrier protein domain of ACP was based on consensus amino acid alignment between ACP orthologues (Fig. S1). Expression of the recombinant/mature ACP (rmACP<sub>68–148</sub>) protein, which is encoded by *acp*<sub>202–444</sub>, was carried out with the following forward and reverse primers, 5'-ACT ATA GAG CGC CTT TGT AAG ATT C-3', and 5'-GAT GTC TTG TCG ACG TTC TAG CTT AC-3'. *Acp*<sub>202–444</sub> gene was PCR-amplified from one of the previously generated clones, using the same PCR conditions described above. PCR product was cloned into a pTrcHis TOPO® TA Expression vector (Invitrogen) and positive clones were confirmed by sequencing. Expression of the His-tagged rmACP<sub>68–148</sub> was induced with a final concentration of 1 mM IPTG and visualized on 4–20% Tris-HCl SDS-PAGE electrophoresis system (Bio-Rad) stained with Coomassie Brilliant Blue R-250. Purification of rmACP<sub>68–148</sub> was carried out using ProBond™ Purification System (Invitrogen) under denaturing condition, followed by electro-elution of gel-embedded rmACP<sub>68–148</sub>. Briefly, after column purification of rmACP<sub>68–148</sub>, fractions were pooled and electrophoresed and the predicted sized band was excised and electro-eluted. The resulting electro-eluted protein was dialyzed to remove residual urea. SDS was also removed using SDS-Out precipitation kit (Pierce). Concentration of rmACP<sub>68–148</sub> was determined using Micro BCA Protein Assay Reagent Kit (Pierce) with bovine serum albumin as a standard. Purified rmACP<sub>68–148</sub> was detected by western blot using rabbit anti-His antibody (Santa Cruz Biotechnology). Antibody production of rmACP<sub>68–148</sub> was subsequently generated (Pacific Immunology Corp., CA), affinity-purified using HiTrap™ Protein A HP Columns (GE Healthcare) and validated by western blot analysis using *B. bovis* infected erythrocytes, uninfected erythrocytes and recombinant ACP. Western blot analysis using pre-immune serum was also performed to ensure specificity of the immune serum.

Determination of the active enzymatic domain of LytB was based on consensus amino acid alignment between four LytB orthologues (Fig. S2). Expression of the recombinant/mature LytB (rmLytB<sub>82–419</sub>) protein, which is encoded by *lytB*<sub>246–1257</sub>, was carried out with the following forward and reverse primers, 5'-AAG ACG GTG TTT TTA TTA GAG CCA CGA GGC-3', and 5'-TGT GCT GAC ACC CGG GCT-3'. *LytB*<sub>246–1257</sub> gene was PCR-amplified from one of the previously generated clones, using the same PCR conditions described above. PCR product was cloned into a pTrcHis TOPO® TA Expression vector (Invitrogen) and selected clones were confirmed by sequencing. The His-tagged rmLytB<sub>82–419</sub> was expressed and purified using the same protocol as described for rmACP<sub>68–148</sub>.

Antibody production of rmLytB<sub>82–419</sub> was subsequently generated (Pacific Immunology Corp., CA), affinity-purified using HiTrap™ Protein A HP Columns (GE Healthcare) and validated for specificity as applied to anti-ACP described above.

## 2.6. Immunofluorescent assay

*B. bovis* culture with 4% parasitized erythrocytes was incubated for 30 min at 37 °C with media containing 400 nM MitoTracker Orange CMTMRos (Invitrogen) for mitochondrial labeling. Cells were washed with fresh media and then centrifuged at 500 × *g* for 1 min. The infected erythrocyte pellet was mixed in a 1:10 ratio with 3% BSA/PBS and thin smears were subsequently prepared. Slides were covered with a 2% paraformaldehyde solution at pH 7.4, fixed for 5 min, and rinsed in 1 × PBS, permeabilized with 0.2% Triton X-100/PBS for 10 min. All steps were performed in a wet chamber at room temperature unless noted. They were then washed twice with 1 × PBS and blocked for 30 min at 37 °C with 3% BSA in PBS. Slides were then incubated with affinity purified anti-ACP rabbit IgG antibody at a 1:40 dilution for 1 h, washed twice with 1 × PBS, and incubated with Alexa-Fluor® 647 goat anti-rabbit at a 1:100 dilution for 1 h (Invitrogen). For the detection of native LytB, dilution of the affinity-purified anti-LytB IgG antibody was at 1:50. Controls include pre-immune serum at 1:30 dilution with the appropriate secondary antibodies, secondary antibodies only and uninfected erythrocytes.

For the detection of GFP-BSD reporter protein in the transfection experiments, anti-GFP antibody conjugated to Alexa Fluor 488 (Invitrogen) at 1:500 dilution was used along with anti-ACP (1:40) or anti-LytB (1:50) antibody and incubation was 30 min. After three washes with 1 × PBS, coverslips were mounted on the slides using Vecta Shield mounting medium containing DAPI (Vecta Laboratories Inc.). Images were collected using a Zeiss LSM 510 META confocal laser scanning microscope equipped with 200 Axiovert inverted microscope using a C-APO 63X/1.2W.

## 2.7. Transient transfection of *B. bovis* infected erythrocytes

Fig. 3 is the schematic diagram of the plasmids used. Green fluorescent protein-blasticidin S deaminase (*gfp-bsd*) fusion gene was amplified from plasmid pTracer-CMV/*bsd* (Cat. No. V883-20, Invitrogen) using GFP *EcoRI* F (5'-CGA GGA ATT CAT GGC CTC CAA AGG AGA AG-3') and BSD *EcoRI* R (5'-CTA TGA ATT CGC CCT CCC ACA CAT AAC CAG-3') primers. The PCR product was then digested with *EcoRI* and cloned into plasmid p4-35-*ef-luc*, replacing the luciferase (*luc*) gene [23]. The resulting plasmid was designated p4-35-*gfp-bsd* (Fig. 3A). The predicted N-terminal bipartite apicoplast leading sequence (signal plus transit peptides, 1–60 amino acids (aa)) of ACP was amplified from *B. bovis* cDNA using primers ACP signal pept (1–22 aa) *EcoRI* F (5'-CTG AGA ATT CAT GAA CGT TGT ATT CCG TAT GCT TAA CCC A-3') and ACP transit pept (23–60 aa) *BglIII* R (5'-GAG AGA TCT CTC AGG TTT GGC-3'). In addition, a modified *gfp-bsd* fusion gene was amplified from plasmid pTracer-CMV/*bsd* this time using the above reverse primer, *Bsd EcoRI* R, and GFP-*BglIII*-noATG F primer (5'-CGA AGA TCT GCC TCC AAA GGA-3'). Both amplicons, no ATG-*gfp-bsd* and SP+TP<sub>ACP</sub> were digested with *BglIII* and ligated to generate the SP+TP<sub>ACP</sub>-*gfp-bsd* fusion gene, which was subsequently digested with *EcoRI* and cloned into the linearized, dephosphorylated p4-35-*ef* plasmid. The resulting plasmid was designated p4-35-SP+TP<sub>ACP</sub>-*gfp-bsd* (Fig. 3B). Similar plasmid constructs were used to generate negative controls, p4-35-SP<sub>ACP</sub>-*gfp-bsd* and p4-35-TP<sub>ACP</sub>-*gfp-bsd* (Fig. 3C and D). All plasmids were purified using the Qiagen endotoxin-free maxiprep kit (Qiagen).

The predicted N-terminal bipartite apicoplast leading sequence (signal plus transit peptides) of LytB was amplified from *B. bovis* cDNA using primers LytB signal pept *EcoRI* F (5'-GGG CGA ATT CAT GCT AAA ATT ATT TTT AAT ACT GCT TTC-3') and LytB transit pept *BglIII* R (5'-CGG CAG ATC TCT CTA CAT TAT CCT GTA TTG GTG-3') and the *gfp-bsd* fusion gene was amplified as previously described. Both amplicons were digested with *BglIII* and ligated to generate the SP+TP<sub>LytB</sub>-*gfp-bsd* fusion gene and subsequently cloned into p4-35-*ef* plasmid. The resulting plasmid was designated p4-35-SP+TP<sub>LytB</sub>-*gfp-bsd* (Fig. 3B). In the same fashion, plasmids p4-35-SP<sub>LytB</sub>-*gfp-bsd* and p4-35-TP<sub>LytB</sub>-*gfp-bsd* were also generated which code independently for the predicted N-terminal signal peptide (SP<sub>LytB</sub>) and transit peptide (TP<sub>LytB</sub>) of *B. bovis* LytB fused to *gfp-bsd*, respectively (Fig. 3C and D). Primers used to amplify SP<sub>LytB</sub> were: LytB signal pept *EcoRI* F (described above) and LytB signal pept *BglIII* R (5'-GCC CAG ATC TTA GAC ACT GTG TAA ATG A-3') and primers used to amplify TP<sub>LytB</sub> were: LytB transit pept *EcoRI*-ATG F (5'-GGC CGA ATT CAT GGT TAT CCA ACA TAT AGG TTA C-3') and LytB transit pept *BglIII* R (described above). All plasmids were purified as described above.

Electroporation of *B. bovis*-infected erythrocytes was performed as described by [23] in a Gene Pulser II apparatus (Bio-Rad) using 0.2 cm cuvettes containing 25 µl filter sterilized cytomix buffer (120 mM KCl, 0.15 mM CaCl<sub>2</sub>, 10 mM K<sub>2</sub>HPO<sub>4</sub>/KH<sub>2</sub>PO<sub>4</sub> pH 7.6, 25 mM HEPES pH 7.6, 2 mM EGTA, 5 mM MgCl<sub>2</sub>, final pH 7.6) plus 100 µg of the corresponding plasmids and 75 µl of washed *B. bovis*-infected erythrocytes to a final volume of 100 µl. Control culture containing mock-transfected *B. bovis*-infected erythrocytes was included. Following electroporation, infected erythrocytes were cultured in 24-well plates as described above. The percentage of parasitized erythrocytes (PPE) was estimated daily by microscopic counting of smears stained with Diff-Quick® (Dade Behring). Successfully transfected *B. bovis* were validated using PCR, RT-PCR, and western blot analysis (data not shown). Localization of GFP-BSD was also determined using immunofluorescent assay 4 h post-transfection as described in Section 2.7.

## 2.8. Electron microscopy

In order to visualize the apicoplast of *B. bovis*, infected erythrocytes were cultured to reach a PPE of ~25%, as described by Levy and Ristic [21]. Infected erythrocytes were isolated from the culture by centrifugation at 350 × *g* for 10 min at 4 °C and then fixed with 2.5% glutaraldehyde in 0.1 M cacodylate buffer with 0.2 M sucrose for 2 h at RT without washing. Following 2 × rinses with 0.1 M cacodylate buffer, samples were post-fixed in 2% osmium tetroxide in 0.1 M cacodylate buffer at 4 °C overnight, rinsed with water and placed in 1% aqueous tannic acid for 1 h. Samples were dehydrated in a graded ethanol series (30–100% 3 ×) infiltrated with acetone and embedded in Spurr's resin. Ultra-thin sections were stained with 2% uranyl acetate and Reynolds lead, and observed using a Philips CM 200 or JEOL 1200EX JEM transmission electron microscope (TEM).

## 2.9. In vitro targeted drug inhibition assay

Drug stock solutions of thiolactomycin (Sigma-Aldrich) and triclosan (Fluka) were prepared in tissue-culture grade dimethyl sulfoxide (DMSO). Fosmidomycin (Invitrogen) and Imidocarb dipropionate (ID) (Imizol® Schering-Plough Animal Health) stocks were prepared in sterile water. Drug stocks were diluted daily to 1 µM, 10 µM, and 100 µM except ID which was diluted to a final concentration of 20 µM using culture media. All drugs were stored in the dark at 4 °C. The final DMSO concentration was 0.1%. Hydroethidine (HE) (Invitrogen) was dissolved in DMSO to a



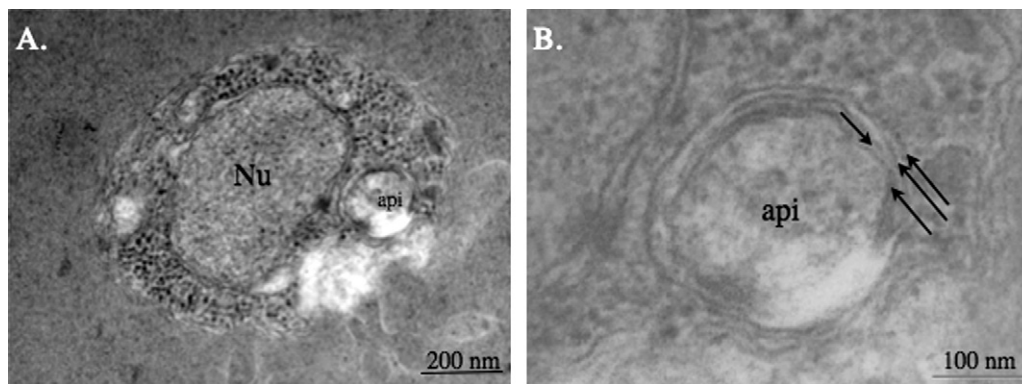


**Fig. 1.** Visualization of *Babesia bovis* apicoplast using transmission electron microscopy. Nu, nucleus and api, apicoplast. (A) illustrates multi-membranous organelle, approximately 200 nm in diameter to be adjacent to the nucleus while (B) is a larger magnification of this organelle surrounded by four membranes, as pointed out by black arrows.

concentration of 10  $\mu\text{g}/\mu\text{l}$  and stored at  $-20^\circ\text{C}$  [24]. Drug inhibition assay was conducted in microaerophilous stationary phase culture in 96-well plates. Each well contained 130  $\mu\text{l}$  of culture at 10% hematocrit with a starting PPE of 0.5 as estimated by microscopic counting of smears stained with Diff-Quick® (Dade Behring). Seventy-five percent of drug containing media was replaced at 24-h intervals. Negative controls included no treatment (NT) and 0.1% DMSO. PPE was enumerated by flow cytometry over a period of 72 h. Briefly, cultures were collected from triplicate wells at 24-h intervals and centrifuged at  $0.4 \times g$  for 5 min to remove media. The cell pellet was resuspended in  $10 \times$  volume of 25  $\mu\text{g}/\mu\text{l}$  HE and incubated at  $37^\circ\text{C}$  for 20 min in the dark. Excess HE was washed from the cells by the addition of  $1 \times$  PBS pH 7.4 followed by centrifugation at  $0.4 \times g$  for 5 min. The cell pellet was resuspended in fresh  $1 \times$  PBS pH 7.4. PPE was then measured by flow cytometry using a Becton Dickinson FACSsort (BD Biosciences) at a flow rate of <2000 events/s with 50,000 events collected. Data was analyzed using FCS Express 3 software (De Novo Software).

### 3. Results/discussion

#### 3.1. Visualization of *Babesia bovis* apicoplast

Complete genome sequencing of *B. bovis* revealed an apicoplast genome [18]. To test whether the intraerythrocytic asexual stage contained a structurally identifiable apicoplast, we used transmission electron microscopy and identified a multi-membranous organelle of approximately 200 nm in diameter (Fig. 1A). There are four membranes surrounding this organelle (Fig. 1B), the same as observed for the apicoplast morphology such as in *Toxoplasma* [25,26], *Garnia* [27] and *Sarcocystis* [28]. The number of membranes surrounding apicoplasts remains somewhat controversial as Hopkins et al. reported that *Plasmodial* apicoplast only contains three membranes [29]. As a result of this discrepancy, questions regarding shared ancestry with dinoflagellates, cryptomonads and heterokonts remains unconfirmed [1].

*B. bovis* apicoplast is located adjacent to the nucleus (Fig. 1A), consistent with potential exchange of molecules between these two compartments [30]. However, we were unable to confirm if the apicoplast reside adjacent to the mitochondrion as well [1], as observed in *Plasmodium*. Multiple attempts were made to localize both the mitochondrion and apicoplast in the same field but were unsuccessful. Thus, our electron microscopy data cannot confirm if *Babesia* mitochondrion is also adjacently positioned to the apicoplast.

#### 3.2. Identification of participants for the *B. bovis* FASII and MEP pathways

The original analysis of the *B. bovis* genome failed to identify the presence of genes encoding proteins involved in FASII biosynthesis, including a gene encoding ACP [18]. However, BLASTP search of the *B. bovis* genome using a consensus ACP active domain compiled from multiple amino acid alignments with seven ACP orthologues identified an *acp*-like gene with 46–85% identity at the deduced amino acid level (Fig. S1). This gene is contained within a larger sequence, BBOV\_I004020, and was initially annotated as encoding only a nucleolar GTP-binding protein 2, missing the *acp*-like sequence. A 476 bp fragment of *acp* was amplified using gDNA. It is predicted to have a small 34 bp intron between nt 287 and 321 (data not shown). *In silico* analysis of the deduced amino acid sequence of *B. bovis* ACP using SignalP ([www.cbs.dtu.dk/services/SignalP](http://www.cbs.dtu.dk/services/SignalP)) predicted a cleavable signal peptide between amino acids (aa) 1 and 22. BLASTP was used to locate the active enzymatic domain which is predicted to initiate around residue 61. This leaves a peptide domain spanning from aa 23 to 60 which may contain a putative transit peptide (TP) (Fig. S1). This putative TP is hydrophobic with 10% of its amino acids being basic in nature. Using RNA isolated from infected erythrocytes, cDNA was generated followed by 5' RACE amplification to identify the 5' untranslated region (UTR) as well as the putative translational start site of ACP. We detected a 442 base pair (bp) *acp* transcript predicted to encode a protein of 18 kDa. 5' RACE amplification identified a 50 bp 5' UTR and two putative translation start sites separated by 15 bp, shown in Fig. S1. Similar BLASTP searches of the *B. bovis* genome using consensus sequences of active domains of the remaining FASII participants failed to identify their orthologues in *B. bovis*. ACP is currently the only FASII pathway participant that has been identified, and shown to be transcribed and translated in *Babesia*. A new GenBank accession no. for *acp* has since been assigned (JN114412). Since ACP is also involved in the respiratory oxidation in mitochondria, ACP detected in *B. bovis* may be mitochondria-associated. However, the presence of the putative signal and transit peptides identified at the amino terminus of the protein, characteristic of a bipartite signal for targeting to the apicoplast, strongly suggests that *B. bovis* ACP likely reside within the apicoplast.

In contrast, the *B. bovis* genome encodes all of the components of the MEP pathway, including LytB. Multiple amino acid sequence alignments of four LytB orthologues subsequently identified the putative reductase domain of *B. bovis* LytB (BBOV.III001660) (Fig. S2). *In silico* analysis using SignalP and BLASTP for the

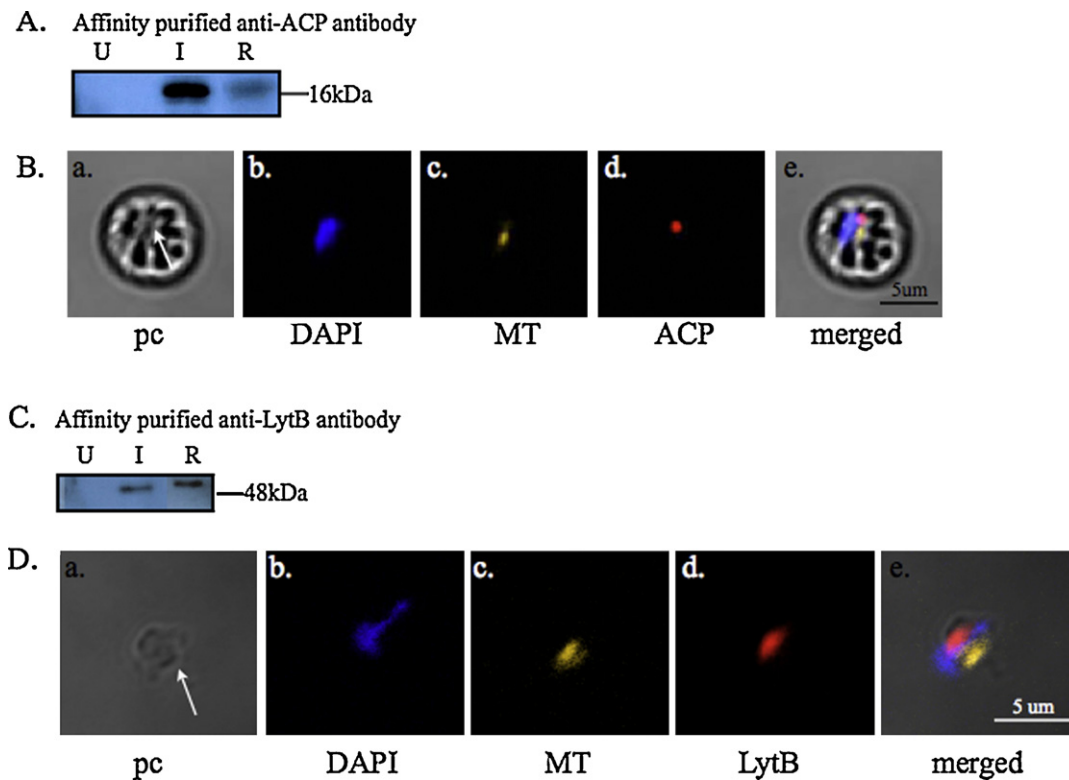


**Fig. 2.** Western blot analysis was used to evaluate specificity of the antibodies raised against the mature active domain of ACP (A) and LytB (C). Affinity-purified anti-ACP or -LytB serum was tested on recombinant protein (R), uninfected (U) and infected (I) erythrocytes. Predicted sized proteins of ~16 kDa and ~48 kDa were detected for ACP and LytB, respectively. Localization of ACP (B) or LytB (D) was illustrated in an infected erythrocyte or free merozoite, respectively. White arrows indicate the location of the parasites. Specific antibody to ACP or LytB recognizes the native protein (d) to lie in a distinct compartment from those of the nucleus, stained with DAPI (b), and the mitochondrion, stained with Mitotracker (MT) (c). (a) and (e) The phase contrast (pc) and merged images, respectively.

predictions of signal peptide and the initiation of the active enzymatic domain, respectively, identified those regions to be between aa 1 and 16, and around aa 72, respectively (Fig. S2). This leaves a putative transit peptide to reside between aa 17 and 71 which is hydrophobic and basic, similar to the TP of ACP. Amplification of *lytB*, which is a gene of 1369 bp with three introns, and its respective 1261 bp transcript, were successful and identical to the predicted sequences previously reported [18] (data not shown).

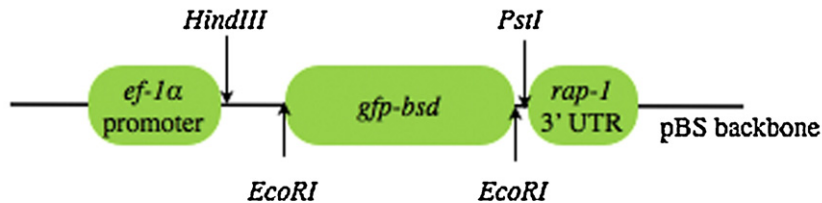
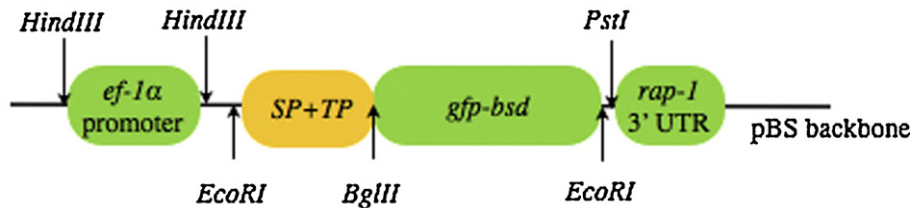
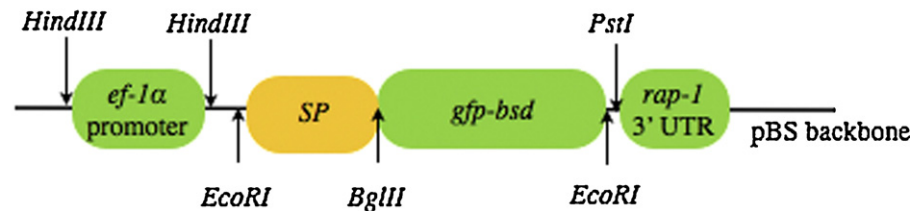
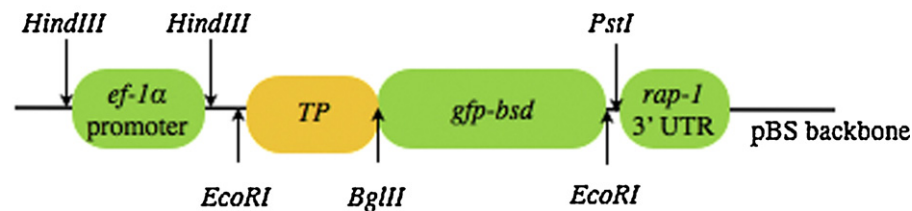
### 3.3. Localization of ACP and LytB

To test whether ACP and LytB are localized to the apicoplast or the mitochondria, polyclonal antibodies were generated against recombinant proteins lacking both the putative signal and transit peptides. Western blot analyses were conducted using infected and uninfected erythrocytes on the immune sera to verify the specificity of the two antibodies (Fig. 2A and C). Predicted sized protein bands corresponding to the native ACP (~16 kDa) and LytB (~48 kDa) were detected in the infected erythrocytes only (Fig. 2A and C, lanes "I"). Preimmune sera were also tested and were unreactive to uninfected and infected erythrocytes as well as the recombinant proteins (data not shown). Mature luminal apicoplast proteins do not contain the signal and transit peptides. Evidence shows that the signal peptide is cleaved prior to apicoplast entry while the transit peptide is cleaved within the lumen [1,31]. For the immunofluorescent assay, the nucleus was labeled with DAPI (Fig. 2B-b and D-b) and the mitochondrion with Mitotracker-Orange (Fig. 2B-c and D-c). Our results demonstrate that ACP and LytB were localized to

a discrete organelle (Fig. 2B-d and D-d). Merged images also suggest that this discrete organelle, presumably the apicoplast, may lie adjacent to the mitochondrion within the parasite (Fig. 2B-e and D-e), a result that our electron microscopy data were unable to confirm. These results also indicate that *B. bovis* does not contain a mitochondrial ACP.

### 3.4. N-terminal bipartite sequence is required for targeting proteins to the apicoplast lumen

*In silico* sequence analysis indicated the presence of putative N-terminal signal (SP) and transit (TP) peptides (bipartite signal) for both ACP and LytB, a prerequisite shared by many nuclear-encoded proteins targeted to the apicoplast in *Plasmodium* and *Toxoplasma* [32]. To test if the bipartite signal is sufficient and required for correct trafficking of proteins to the apicoplast, *B. bovis* was transfected with SP+TP<sub>ACP</sub>-GFP-BSD or SP+TP<sub>LytB</sub>-GFP-BSD expression cassette (Fig. 3B). Controls included constructs that only contain SP<sub>ACP</sub>, SP<sub>LytB</sub>, TP<sub>ACP</sub> or TP<sub>LytB</sub>. Mock transfection using p4-35-GFP-BSD was the negative control. Immunofluorescent assays performed 4 h post-transfection revealed the localization of GFP (Fig. 4A and B) in an organelle distinct from the nucleus and mitochondrion; the fluorescence staining of the GFP (Fig. 4A-e and B-j) was similar to that of the native ACP (Fig. 4A-d) and LytB (Fig. 4B-i), respectively, suggesting that both GFP and ACP or LytB reside in the same compartment. In contrast, neither SP nor TP alone, as illustrated by constructs SP<sub>LytB</sub>+GFP or TP<sub>LytB</sub>+GFP, directed GFP into the same compartment as the native LytB (Fig. 4C and D). Similar results were also obtained using constructs containing

A. p4-35-*gfp-bsd*:B. p4-35-SP+TP<sub>ACP</sub> or LylB-*gfp-bsd*:C. p4-35-SP<sub>ACP</sub> or LylB-*gfp-bsd*:D. p4-35-TP<sub>ACP</sub> or LylB-*gfp-bsd*:

**Fig. 3.** Schematic diagram of the constructs used in a series of *Babesia bovis* transient transfections. Controls include (A) plasmid with no bipartite sequence, (B) plasmid containing the bipartite sequence and the reporter cassette (GFP), (C) two plasmids, SP<sub>ACP</sub> + GFP and SP<sub>LylB</sub> + GFP and (D) two plasmids, TP<sub>ACP</sub> + GFP and TP<sub>LylB</sub> + GFP.

SP<sub>ACP</sub> + GFP or TP<sub>ACP</sub> + GFP (data not shown). Construct consisting only of the reporter cassette also did not direct GFP into the apicoplast as expected (Fig. 4E). These data collectively indicate that the complete bipartite signal (SP and TP) is necessary and sufficient for correct apicoplast trafficking.

### 3.5. Pharmacologic inhibition

Based on our genomic analyses of pathway composition and consequent expression data, we predicted that a functional MEP pathway exists within *B. bovis* while a functional FASII pathway does not. To determine the presence or absence of these two pathways, fosmidomycin was used to target MEP biosynthesis while thiolactomycin, triclosan and isoniazid were used to target FASII pathway. Fosmidomycin inhibits the action of DOXP reductoisomerase, blocking the conversion of DOXP to 2-C-methyl-D-erythritol 4-phosphate. Fosmidomycin also

interacts indirectly with methylerythritol phosphate cytidyltransferase (IspD), an enzyme immediate downstream of DOXP reductoisomerase [33]. Thiolactomycin targets ketoacyl-ACP synthase (Fab B/F) in *P. falciparum* [34] while triclosan targets enoyl-acyl carrier protein reductase (Fab I) [35–37].

Fosmidomycin was effective in the inhibition of *B. bovis* growth after 24 h at concentrations  $\geq 10 \mu\text{M}$  (Fig. 5C). This effect has also been reported in *P. falciparum*, albeit at lower dosages [38]. The inhibitory effect of fosmidomycin on *B. bovis* indicates that its substrate(s) is/are present and further suggests that the MEP pathway is functional and required for intraerythrocytic growth of the asexual stages. In contrast, inhibition of the FASII pathway using thiolactomycin at concentrations between  $1 \mu\text{M}$  and  $100 \mu\text{M}$  showed no significant inhibition of *B. bovis* growth (Fig. 5A). Triclosan failed to inhibit *B. bovis* growth at  $1 \mu\text{M}$  and  $10 \mu\text{M}$  concentrations; while growth was inhibited with  $100 \mu\text{M}$

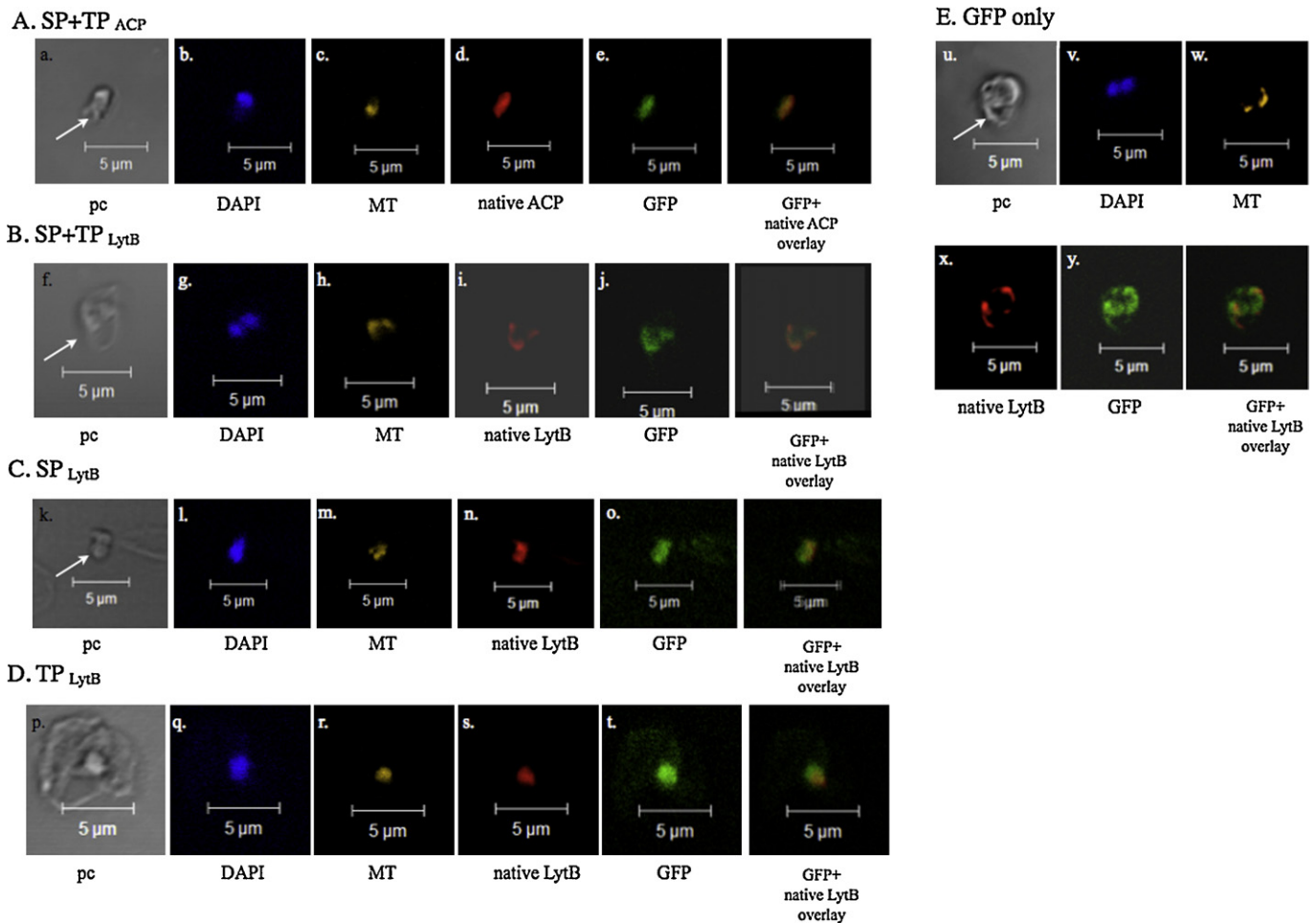


**Fig. 4.** Immunofluorescent assay to detect *Babesia bovis* that were transiently transfected with (A) SP+TP<sub>ACP</sub>, (B) SP+TP<sub>LytB</sub>, (C) SP<sub>LytB</sub>, (D) TP<sub>LytB</sub> or (E) GFP only. Detection of GFP was carried out using an anti-GFP antibody conjugated with Alexa Fluor 488. Using construct in (A) and (B), GFP localizes to a compartment as the native ACP (d, e) or LytB (i, j). In contrast, constructs containing only SP or TP, GFP fluorescence extends beyond the compartment where native ACP and LytB reside (C and D). pc, phase contrast; MT, mitotracker stained mitochondrion and DAPI stains nucleus. White arrows show free merozoites while (p) is a *B. bovis* infected erythrocyte. (E) represents a *B. bovis* transfected with a construct that lacks bipartite signal.

triclosan (Fig. 5B), consistent with previous results [39]. However, despite earlier reports that claimed specific activity of triclosan, a recent study demonstrated nonspecific disruption of subcellular membrane structure at high concentrations [40]. Thus, the action of triclosan at 100 μM on *B. bovis* may not be Fab I-specific.

Together the genomic, expression, and pharmacologic data illustrate that significant differences may exist in apicomplexan parasites. Specifically, a complete MEP pathway is likely to be present and functional in the asexual erythrocytic stages of *B. bovis*, similar to that of the asexual erythrocytic stages of *P. falciparum*. DOXP reductoisomerase is actively transcribed during the asexual blood stage (manuscript in prep.), further evidence supporting an active MEP pathway within *B. bovis*. The effectiveness of fosmidomycin may be due to the presence of new permeability pathways (NPP) found in erythrocytes. NPP alters the integrity of the red cell membranes [41,42]. This allows the trafficking of fosmidomycin to be effective against apicomplexans such as *Plasmodium* which resides within erythrocytes. In contrast, *Toxoplasma*, *Theileria* and *Eimeria* have all been reported to contain genes involved in MEP pathway and yet are non-responsive to fosmidomycin, even at 400 μM [43–46]. Nair et al. recently shown that an apicoplast phosphate translocator (APT)

located on the plasma membrane of the parasites is required to traffic fosmidomycin [46].

In contrast, a complete FASII pathway is probably lacking in *B. bovis* with only the presence of ACP. Consistent with this absence of the complete pathway, pharmacological inhibition within the specific inhibitor range had no effect on intraerythrocytic growth of *B. bovis* asexual stages. This lack of a functional requirement for the FASII pathway in asexual erythrocytic stages is supported by the lack of expression of FASII pathway participants (except ACP) and sensitivity to inhibition of this pathway in the erythrocytic stages of *P. falciparum* [14,15]. However, unlike *B. bovis* which only has the intraerythrocytic stages in the mammalian host, *P. falciparum* has a complete FASII pathway which is required for growth in the hepatic stages. These observations are consistent with specific molding of apicomplexan pathways to meet the specific requirements of apicomplexan parasites, requirements which differ in a stage-specific/host cell-specific manner. *P. falciparum* retained the pathway for those stages where it was required but regulated expression in the asexual erythrocytic stages where the pathway is not needed. In the case of *Babesia*, *B. bovis* may have lost most of the pathway components as it adapts to asexual stage growth within mature erythrocytes. Thus, the apicoplast residing ACP may be the final footprint of a once functional FASII pathway which will soon be lost through evolution.



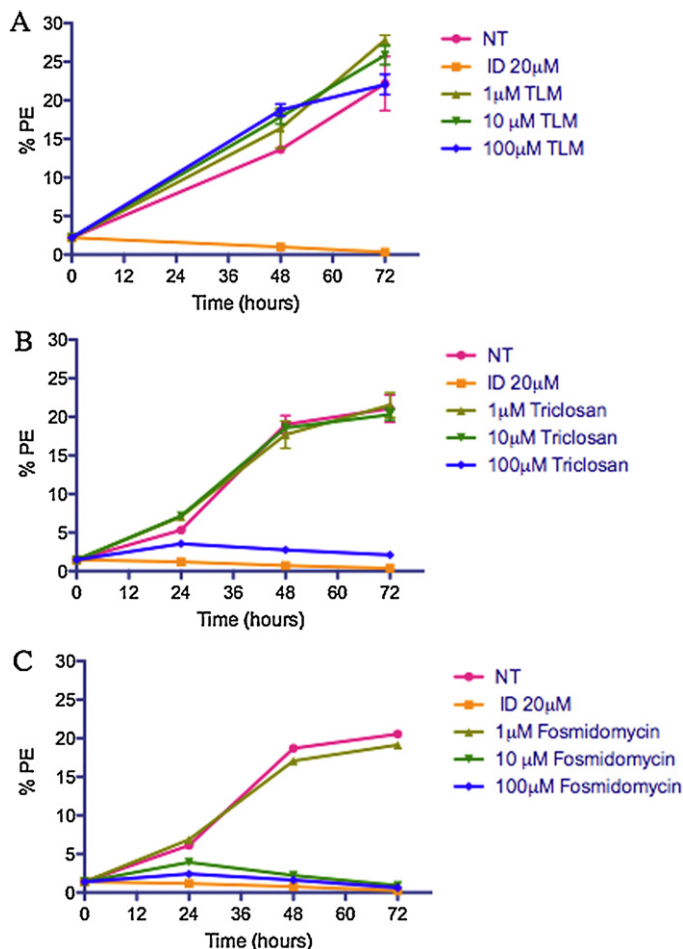


**Fig. 5.** In vitro *Babesia bovis* growth inhibition assay using 1, 10 and 100 µM thiolactomycin (TLM) (A), triclosan (B) and fosmidomycin (C) over 72 h. Experiments were conducted in triplicates. Controls include no treatment (NT) and imidocarb dipropionate (ID) at a final concentration of 20 µM. %PE, percent parasitized erythrocytes.

## Acknowledgements

We would like to thank Dr. David Schneider, USDA-ARS, Pullman WA for his expertise on fluorescent experiment optimization; David Herndon for maintenance of *B. bovis* culture; Paul Lacy, Jacob Laughery and Tracy Luu for their assistances in this project. This work is partly funded by WSU College of Veterinary Medicine intramural grants, Wellcome Trust GRO075800M and USDA-ARS Cooperative Agreement 58-5348-7-528.

## Appendix A. Supplementary data

Supplementary data associated with this article can be found, in the online version, at [doi:10.1016/j.molbiopara.2011.10.009](https://doi.org/10.1016/j.molbiopara.2011.10.009).

## References

- [1] Waller RF, McFadden GI. The apicoplast: a review of the derived plastid of apicomplexan parasites. *Curr Issues Mol Biol* 2005;7(1):57–79.
- [2] Foth BJ, McFadden GI. The apicoplast: a plastid in *Plasmodium falciparum* and other Apicomplexan parasites. *Int Rev Cytol* 2003;224:57–110.
- [3] Lau AO, McElwain TF, Brayton KA, Knowles DP, Roalson EH. *Babesia bovis*: a comprehensive phylogenetic analysis of plastid-encoded genes supports green algal origin of apicoplasts. *Exp Parasitol* 2009;123(3):236–43.
- [4] Hirt RP, Horner DS. Organelles, genomes, and eukaryote phylogeny: an evolutionary synthesis in the age of genomics. Boca Raton: CRC Press; 2004.
- [5] Williams BA, Keeling PJ. Cryptic organelles in parasitic protists and fungi. *Adv Parasitol* 2003;54:9–68.
- [6] Mazumdar J, Striepen B. Make it or take it: fatty acid metabolism of apicomplexan parasites. *Eukaryot Cell* 2007;6(10):1727–35.
- [7] Mazumdar J, E HW, Masek K, C AH. Striepen B: apicoplast fatty acid synthesis is essential for organelle biogenesis and parasite survival in *Toxoplasma gondii*. *Proc Natl Acad Sci USA* 2006;103(35):13192–7.
- [8] Waller RF, Keeling PJ, Donald RG, Striepen B, Handman E, Lang-Unnasch N, et al. Nuclear-encoded proteins target to the plastid in *Toxoplasma gondii* and *Plasmodium falciparum*. *Proc Natl Acad Sci USA* 1998;95(21):12352–7.
- [9] Sackmann U, Zensen R, Rohlen D, Jahnke U, Weiss H. The acyl-carrier protein in *Neurospora crassa* mitochondria is a subunit of NADH:ubiquinone reductase (complex I). *Eur J Biochem* 1991;200(2):463–9.
- [10] Chuman L, Brody S. Acyl carrier protein is present in the mitochondria of plants and eucaryotic micro-organisms. *Eur J Biochem* 1989;184(3):643–9.
- [11] Sacchetti JC, Poulter CD. Creating isoprenoid diversity. *Science* 1997;277(5333):1788–9.
- [12] Rohmer M. The discovery of a mevalonate-independent pathway for isoprenoid biosynthesis in bacteria, algae and higher plants. *Nat Prod Rep* 1999;16(5):565–74.
- [13] Rohdich F, Hecht S, Gartner K, Adam P, Krieger C, Amslinger S, et al. Studies on the nonmevalonate terpene biosynthetic pathway: metabolic role of IsppH (LytB) protein. *Proc Natl Acad Sci USA* 2002;99(3):1158–63.
- [14] Yu M, Kumar TR, Nkrumah LJ, Coppi A, Retzlaff S, Li CD, et al. The fatty acid biosynthesis enzyme FabI plays a key role in the development of liver-stage malarial parasites. *Cell Host Microbe* 2008;4(6):567–78.
- [15] Vaughan AM, O'Neill MT, Tarun AS, Camargo N, Phuong TM, Aly AS, et al. Type II fatty acid synthesis is essential only for malaria parasite late liver stage development. *Cell Microbiol* 2009;11(3):506–20.
- [16] Ralph SA, Van Dooren GG, Waller RF, Crawford MJ, Fraunholz MJ, Foth BJ, et al. Tropical infectious diseases: metabolic maps and functions of the *Plasmodium falciparum* apicoplast. *Nat Rev Microbiol* 2004;2(3):203–16.
- [17] Lu JZ, Muench SP, Allary M, Campbell S, Roberts CW, Mui E, et al. Type I and type II fatty acid biosynthesis in *Eimeria tenella*: enoyl reductase activity and structure. *Parasitology* 2007;134(Pt.14):1949–62.
- [18] Brayton KA, Lau AO, Herndon DR, Hannick L, Kappmeyer LS, Berens SJ, et al. Genome sequence of *Babesia bovis* and comparative analysis of apicomplexan hemoprotozoa. *PLoS Pathog* 2007;3(10):1401–13.
- [19] Rodriguez SD, Buening GM, Green TJ, Carson CA. Cloning of *Babesia bovis* by in vitro cultivation. *Infect Immun* 1983;42(1):15–8.
- [20] Hines SA, McElwain TF, Buening GM, Palmer GH. Molecular characterization of *Babesia bovis* merozoite surface proteins bearing epitopes immunodominant in protected cattle. *Mol Biochem Parasitol* 1989;37(1):1–9.
- [21] Levy MG, Ristic M. *Babesia bovis*: continuous cultivation in a microaerophilous stationary phase culture. *Science* 1980;207(4436):1218–20.
- [22] Goff WL, Yunker CE. *Babesia bovis*: increased percentage parasitized erythrocytes in cultures and assessment of growth by incorporation of [3H]hypoxanthine. *Exp Parasitol* 1986;62(2):202–10.
- [23] Suarez CE, McElwain TF. Transient transfection of purified *Babesia bovis* merozoites. *Exp Parasitol* 2008;118(4):498–504.
- [24] Davis WC, Wyatt CR, Hamilton MJ, Goff WL. A rapid, reliable method of evaluating growth and viability of intraerythrocytic protozoan hemoparasites using fluorescence flow cytometry. *Mem Inst Oswaldo Cruz* 1992;87(Suppl. 3):235–9.
- [25] Kohler S, Delwiche CF, Denny PW, Tilney LG, Webster P, Wilson RJ, et al. A plastid of probable green algal origin in Apicomplexan parasites. *Science* 1997;275(5305):1485–9.
- [26] McFadden GI, Roos DS. Apicomplexan plastids as drug targets. *Trends Microbiol* 1999;7(8):328–33.
- [27] Diniz JA, Silva EO, Lainson R, de Souza W. The fine structure of *Garnia gonadati* and its association with the host cell. *Parasitol Res* 2000;86(12):971–7.
- [28] Tomova C, Geerts WJ, Muller-Reichert T, Entzeroth R, Humbel BM. New comprehension of the apicoplast of *Sarcocystis* by transmission electron tomography. *Biol Cell* 2006;98(9):535–45.
- [29] Hopkins J, Fowler R, Krishna S, Wilson I, Mitchell G, Bannister L. The plastid in *Plasmodium falciparum* asexual blood stages: a three-dimensional ultrastructural analysis. *Protist* 1999;150(3):283–95.
- [30] Lim L, McFadden GI. The evolution, metabolism and functions of the apicoplast. *Philos Trans R Soc Lond B: Biol Sci* 2010;365(1541):749–63.
- [31] van Dooren GG, Su V, D'Ombra MC, McFadden GI. Processing of an apicoplast leader sequence in *Plasmodium falciparum* and the identification of a putative leader cleavage enzyme. *J Biol Chem* 2002;277(26):23612–9.
- [32] Harb OS, Chatterjee B, Fraunholz MJ, Crawford MJ, Nishi M, Roos DS. Multiple functionally redundant signals mediate targeting to the apicoplast in the apicomplexan parasite *Toxoplasma gondii*. *Eukaryot Cell* 2004;3(3):663–74.
- [33] Zhang B, Watts KM, Hodge D, Kemp LM, Hunstad DA, Hicks LM, et al. A second target of the antimalarial and antibacterial agent fosmidomycin revealed by cellular metabolite profiling. *Biochemistry* 2011;50(17):3570–7.
- [34] Waller RF, Ralph SA, Reed MB, Su V, Douglas JD, Minnikin DE, et al. A type II pathway for fatty acid biosynthesis presents drug targets in *Plasmodium falciparum*. *Antimicrob Agents Chemother* 2003;47(1):297–301.
- [35] Bhat GP, Suroli A. Triclosan and fatty acid synthesis in *Plasmodium falciparum*: new weapon for an old enemy. *J Biosci* 2001;26(1):1–3.
- [36] Kapoor M, Gopalakrishnapai J, Suroli A, Suroli A. Mutational analysis of the triclosan-binding region of enoyl-ACP (acyl-carrier protein) reductase from *Plasmodium falciparum*. *Biochem J* 2004;381(Pt 3):735–41.
- [37] Lu H, Tonge PJ. Inhibitors of FabI, an enzyme drug target in the bacterial fatty acid biosynthesis pathway. *Acc Chem Res* 2008;41(1):11–20.



- [38] Jomaa H, Wiesner J, Sanderbrand S, Altincicek B, Weidemeyer C, Hintz M, et al. Inhibitors of the nonmevalonate pathway of isoprenoid biosynthesis as antimalarial drugs. *Science* 1999;285(5433):1573–6.
- [39] Bork S, Yokoyama N, Matsuo T, Claveria FG, Fujisaki K, Igarashi I. Growth inhibitory effect of triclosan on equine and bovine Babesia parasites. *Am J Trop Med Hyg* 2003;68(3):334–40.
- [40] Paul KS, Bacchi CJ, Englund PT. Multiple triclosan targets in *Trypanosoma brucei*. *Eukaryot Cell* 2004;3(4):855–61.
- [41] Kirk K. Membrane transport in the malaria-infected erythrocyte. *Physiol Rev* 2001;81(2):495–537.
- [42] Baumeister S, Wiesner J, Reichenberg A, Hintz M, Bietz S, Harb OS, et al. Fosmidomycin uptake into Plasmodium and babesia-infected erythrocytes is facilitated by parasite-induced new permeability pathways. *PLoS ONE* 2011;6(5):e19334.
- [43] Clastre M, Goubard A, Prel A, Mincheva Z, Viaud-Massuati MC, Bout D, et al. The methylerythritol phosphate pathway for isoprenoid biosynthesis in coccidia: presence and sensitivity to fosmidomycin. *Exp Parasitol* 2007;116(4):375–84.
- [44] Nair SC, Brooks CF, Goodman CD, Strum A, McFadden GI, Sundriyal S, et al. Apicoplast isoprenoid precursor synthesis and the molecular basis of fosmidomycin resistance in *Toxoplasma gondii*. *J Exp Med* 2011;208(7):1547–59.
- [45] Lizundia R, Werling D, Langsley G, Ralph SA. Theileria apicoplast as a target for chemotherapy. *Antimicrob Agents Chemother* 2009;53(3):1213–7.
- [46] Nair SC, Brooks CF, Goodman CD, Strum A, McFadden GI, Sundriyal S, et al. Apicoplast isoprenoid precursor synthesis and the molecular basis of fosmidomycin resistance in *Toxoplasma gondii*. *J Exp Med* 2011;208(7):1547–59.